Article

Not peer-reviewed version

Rapoport's Rule, Ecotone Concept, and Salinity Gradient Predict the Distribution of Benthic Foraminifera in a Southeastern Pacific Estuary

Leonardo D. Fernández * and Margarita Marchant

Posted Date: 13 December 2024

doi: 10.20944/preprints202412.1159.v1

Keywords: beta diversity; foraminifers, estuarine gradient; microbial biogeography; mid-domain effect; aquatic protists, Rapoport effect; turnover; source-sink dynamics; unicellular eukaryotes

 doi:10.20944/preprints202412.1159.v1

Article

Rapoport's Rule, Ecotone Concept, and Salinity Gradient Predict the Distribution of Benthic Foraminifera in a Southeastern Pacific Estuary

Leonardo D. Fernández [1,*] and Margarita Marchant [2]

[1] Núcleo de Investigación en Sustentabilidad Agroambiental (NISUA), Facultad de Medicina Veterinaria y Agronomía, Universidad de Las Américas, Manuel Montt 948, Providencia, Santiago, Chile; limnoleo@gmail.com

[2] Departamento de Zoología, Universidad de Concepción, Concepción, Chile; mmarchan@udec.cl

* Correspondence: limnoleo@gmail.com

Abstract: This study explores the biogeographic processes shaping the distribution of benthic foraminifera along a salinity gradient in the Contaco Estuary, southeastern Pacific, Chile. The primary aim was to evaluate the applicability of key ecological paradigms—Rapoport's rule, the mid-domain effect, ecotones, and source-sink dynamics—to unicellular eukaryotes in estuarine environments. A 1,550 m longitudinal transect, sampled at 50 m intervals, revealed a pronounced salinity-driven pattern in species richness and diversity, with calcareous taxa dominating euhaline zones and agglutinated taxa thriving in brackish and freshwater areas. Source-sink dynamics was not supported, as beta diversity analyses identified turnover as the dominant driver, highlighting species replacement along the salinity gradient. Evidence of a longitudinal Rapoport effect was observed, with broader distribution ranges in low-salinity environments, reflecting adaptations to suboptimal conditions. Contrary to predictions, the mid-domain effect was not supported, as foraminiferal richness showed a monotonic decline. These findings extend macroecological principles to microbial communities, emphasizing deterministic processes in shaping estuarine diversity. This research provides a robust framework for understanding biodiversity patterns in dynamic ecosystems, offering valuable insights for conservation and ecological monitoring.

Keywords: beta diversity; foraminifers; estuarine gradient; microbial biogeography; mid-domain effect; aquatic protists; Rapoport effect; turnover; source-sink dynamics; unicellular eukaryotes

1. Introduction

Understanding patterns of diversity and their underlying processes is a central goal in ecology. These patterns, which describe how species richness and composition vary across spatial or environmental gradients, are often shaped by ecological mechanisms such as niche differentiation, environmental filtering, or dispersal limitations [1]. Among multicellular eukaryotes like plants and animals, well-documented processes such as source-sink dynamics, Rapoport's rule, and the mid-domain effect have been proposed to explain diversity patterns along geographic or environmental gradients [2–9]. However, whether these processes also govern the diversity patterns of unicellular eukaryotes (protists) remains an open question [10–15].

Estuarine benthic foraminifera serve as an excellent model for investigating diversity patterns and their drivers in protists. These heterotrophic eukaryotes are characterized by their reticulopodia or axopodia and their multi-chambered tests or shells [16]. Two types of benthic foraminiferal taxa are typically observed in estuaries: calcareous species, which are highly dependent on available calcium carbonate to construct their shells [17,18], and agglutinated species, which rely less on calcium carbonate as they use it only as a binding agent to cement sediment particles into their shells

 doi:10.20944/preprints202412.1159.v1

[18,19]. These contrasting physiological requirements make benthic foraminifera particularly sensitive to salinity gradients, a defining feature of estuaries [20,21].

Globally, the distribution of benthic foraminifera in estuaries follows a predictable pattern where species richness decreases progressively from the marine to the freshwater realm [20,22]. This trend is typically accompanied by the formation of three distinct communities along the salinity gradient [21,23]. The first, located near the estuary mouth, is dominated by calcareous taxa adapted to high-salinity environments. The second, at the estuary head, consists predominantly of agglutinated taxa capable of thriving in low-salinity conditions. Between these two zones lies a transitional community, or ecotone, where calcareous and agglutinated species overlap. This ecotone reflects the mixing of marine and freshwater influences, with species adapted to intermediate salinity levels, creating a unique assemblage that bridges the more homogeneous communities at either end of the gradient [20–23]. While this "transitional assemblage pattern" (TA-pattern) has been well-studied in Northern Hemisphere estuaries [20–22], little is known about whether it applies to estuaries in historically understudied regions, such as the southeastern Pacific coastline [24–27].

At least three ecological mechanisms have been proposed to explain similar diversity gradients in multicellular eukaryotes [2–6], and their potential applicability to protists is worth exploring. First, **Rapoport's rule** posits that species inhabiting favorable environments (e.g., the mouth of an estuary), often have narrower environmental tolerances and smaller distribution ranges, supporting higher species richness of specialist taxa [28,29]. In contrast, species in less favorable environments (e.g., the head of an estuary) tend to have broader environmental tolerances and larger distribution ranges, resulting in fewer species but with wider ecological niches [28,29]. This macroecological rule suggests that the ecological constraints imposed by environmental variability play a key role in shaping species richness and distribution patterns along environmental gradients [5]. Second, source-sink dynamics describe how species-rich communities in favorable habitats (sources) support the persistence of species in less favorable, species-poor habitats (sinks) through immigration. This mechanism predicts a nested pattern of species distribution where communities in low-quality habitats are mere subsets of those in high-quality habitats [30,31]. Third, the mid-domain effect (MDE) predicts a hump-shaped pattern of species richness driven by geometric constraints: the random overlap of species ranges within a bounded domain (e.g., an estuary) results in higher richness in the center of the domain and lower richness near its boundaries [32,33].

Additionally, the debate surrounding the drivers of diversity patterns in estuarine microbes remains unresolved. Do environmental gradients, such as salinity, drive diversity and composition through deterministic processes, or do stochastic mechanisms dominate [14,34]. Testing (macro)ecological hypotheses like Rapoport's rule or the MDE in estuarine protists offers a unique opportunity to explore these questions and assess whether the processes shaping the diversity of macroorganisms are also relevant for unicellular eukaryotes [11,35].

In this study, we aim to fill these knowledge gaps by investigating the diversity and distribution of benthic foraminifera in the Contaco River estuary, a temperate estuary located in the southeastern Pacific, Chile. Although there are some studies on protists [36,37] and benthic foraminifera along the Chilean coastline [38–48], research on estuarine benthic foraminifera is limited [24–27,49]. This limited body of work underscores the precarious state of knowledge regarding these organisms in estuarine environments, making the Contaco River estuary an ideal setting to test macroecological hypotheses in protists. Specifically, we address two objectives: (1) to describe the diversity and distribution of benthic foraminifera along a salinity gradient in the estuary; and (2) to evaluate the applicability of key ecological concepts, including Rapoport's rule, source-sink dynamics, the TA-pattern, and the mid-domain effect, in explaining observed diversity patterns.

2. Materials and Methods

2.1. Study Area

The Contaco River, located in the Los Lagos Region of southern Chile, spans 48 km and originates at ~900 m above sea level (a.s.l.) in the Chilean Coastal Range. The river flows into the

 doi:10.20944/preprints202412.1159.v1

Pacific Ocean near Pucatrihue (Figure 1). The region experiences a temperate Mediterranean-type climate with annual precipitation exceeding 2,000 mm, driven by the prevailing westerly system and the presence of the Andes and Coastal Mountain ranges [25]. The Contaco River's steep slope and constant freshwater inputs from rainfall, groundwater, and surface runoff restrict the salt wedge's influence to approximately 1,500 m upstream, classifying it as a microtidal estuary [24].

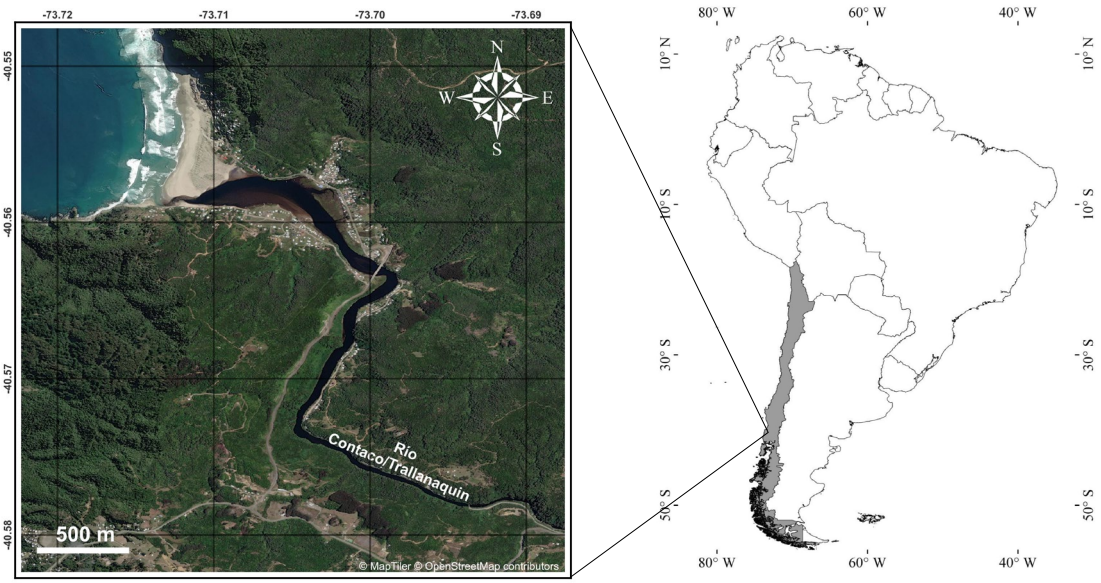

Figure 1. Location of the Contaco Estuary on the southeastern Pacific coast of Chile. The left panel shows a high-resolution satellite view of the estuary and its surrounding area. The right panel highlights the position of the estuary in Chile (shaded gray) within South America. Map data © OpenStreetMap contributors and MapTiler.

2.2. Sampling of Benthic Foraminifera

In January 2018, 32 surface sediment samples were collected along a ~1,550 m longitudinal transect covering the estuary from its mouth to its headwaters. Sampling sites were spaced ~50 m apart, and 10 cm^3 of sediment were retrieved from the center of the estuarine channel using SCUBA diving. This method ensures minimal disturbance to sediment layers, allowing for accurate quantification of foraminiferal populations [21,50].

Each sediment sample was immediately preserved in vials containing a solution of distilled water (70%), ethanol (30%), and Rose Bengal stain (1.5 g/L), along with 0.5 g of sodium carbonate. Rose Bengal was used to differentiate living specimens, stained at the time of collection, from dead ones [51,52]. Samples were processed within 3–4 days, washed through 500 µm and 63 µm mesh sieves, and suspended in 500 mL of water [21,50]. Subsamples were prepared to ensure sufficient splits for counting at least 300 individuals (live and dead) [52]. Counts were extrapolated to the total sample volume, and the most abundant species were imaged via scanning electron microscopy (SEM).

Species identification was based on shell morphology following taxonomic guides for southern hemisphere benthic foraminifera [24–48]. Diversity was quantified using the Shannon–Wiener index calculated in PAST v1.5 software [53]. Species richness, defined as the total number of species per site, and relative abundance data were used in all subsequent analyses, focusing exclusively on live specimens.

2.3. Salinity Measurements

Salinity was measured at each sampling site using a multiparameter probe. Measurements were taken at the water-sediment interface to capture conditions relevant to benthic foraminifera, which

 doi:10.20944/preprints202412.1159.v1

inhabit primarily infaunal habitats [21]. Four measurements per site (two at high tide, two at low tide) were averaged to calculate mean salinity over a full tidal cycle. Sampling sites were classified as euhaline (30–40 psu), brackish (0.5–29 psu), or freshwater (< 0.5 psu) [54]. Salinity was with richness, diversity, and abundance benthic foraminifera using linear regressions. Statistical inferences were performed using EcoSim v7.68 [55] with 50,000 randomized matrices.

2.4. Evaluation of Sampling Artifacts

Rarefaction-extrapolation curves were generated using the package iNEXT [56] with 1,000 permutations. This analysis evaluated the adequacy of sampling effort and the proportion of species detected based on the seamless rarefaction and extrapolation sampling curves of Hill numbers for q = 0 [56].

2.5. Assessing the Longitudinal Rapoport's Rule and Mid-Domain Effect

To test for a longitudinal Rapoport's rule, we analyzed the relationship between species' longitudinal range extent and range midpoint (both log-transformed) using the midpoint method [57]. A positive relationship between these two variables would support the observation of a longitudinal Rapoport's rule [2].

To evaluate the mid-domain effect (MDE), we used the Monte Carlo-based Mid-Domain Null model [58] with 50,000 simulations to compare observed species richness against null-model predictions. A strong fit between observed and predicted richness curves would support the MDE hypothesis [4].

2.6. Testing the TA-Pattern and Source-Sink Dynamics

The TA-pattern predicts that beta diversity, or spatial variation in species composition, arises primarily from turnover, i.e., the replacement of species between euhaline, brackish, and freshwater zones [20,21]. Conversely, source-sink dynamics suggest that spatial variation is driven by nestedness, reflecting a gradual loss of species along an environmental gradient [30,31]. Under this scenario, less diverse sites contain a subset of the species present in more diverse sites [10]. While these two phenomena are not mutually exclusive, one often predominates [12]. To assess the drivers of beta diversity in foraminiferal communities, we analyzed the contributions of turnover and nestedness using the package betapart [59]. A predominance of turnover would support the TA-pattern, whereas dominance of nestedness would indicate the influence of source-sink dynamics on the longitudinal distribution of foraminifera.

To investigate the potential presence of discrete communities predicted by the TA-pattern, we performed several complementary analyses. First, a hierarchical cluster analysis was conducted using the Bray-Curtis dissimilarity index calculated from the species abundance matrix. Clustering was achieved through the group average method, implemented using the hclust() function in base R [60].

We further assessed site dissimilarities through non-metric multidimensional scaling (NMDS) using the Bray-Curtis dissimilarity index. This analysis was conducted with the vegan package [61], configured to explore two dimensions (k = 2 and allow up to 100 iterations for convergence. Stress values below 0.2 indicated an acceptable fit for the ordination. To visualize potential groupings, 95% confidence ellipses were constructed around sampling sites using principal component analysis (PCA) applied to the NMDS coordinates. The ellipses were generated with the ggplot2 package [62], facilitating clear visualization of the relationships among sites.

To statistically test for the significance of observed patterns, we performed two distinct Analysis of Similarity (ANOSIM) tests using the vegan package [61], each with 1,000 permutations. The first ANOSIM used salinity categories (euhaline, brackish, and freshwater) as factors to evaluate the existence of the three communities predicted by the TA-pattern. The second ANOSIM assessed the significance of the clusters identified by the hierarchical clustering and NMDS analyses, confirming whether these groups were significantly distinct. For both tests, the R statistic and associated p-values were used to interpret the significance of the results.

 doi:10.20944/preprints202412.1159.v1

Finally, observed species richness gradients were compared with null model predictions to detect zones of high species richness indicative of transitional assemblages. Null model simulations were conducted using PAST v1.5 software [53], with 1,000 iterations to estimate confidence intervals. Observed richness values were then compared to null expectations to evaluate significant deviations from random patterns.

3. Results

3.1. Salinity Gradient and Foraminiferal Diversity

Salinity significantly decreased with increasing distance from the estuary mouth ($r^2 = 0.382$, $P < 0.0001$; Figure 2), ranging from a maximum of 34.2 psu to a minimum of 0.2 psu along the estuarine gradient. Sampling sites were classified into three water types based on salinity: euhaline (sites 1–4), brackish (sites 5–19, 21, 24–25), and freshwater (sites 20, 22–23, 26–32) (Figure 2). Detailed salinity values are provided in Table S1.

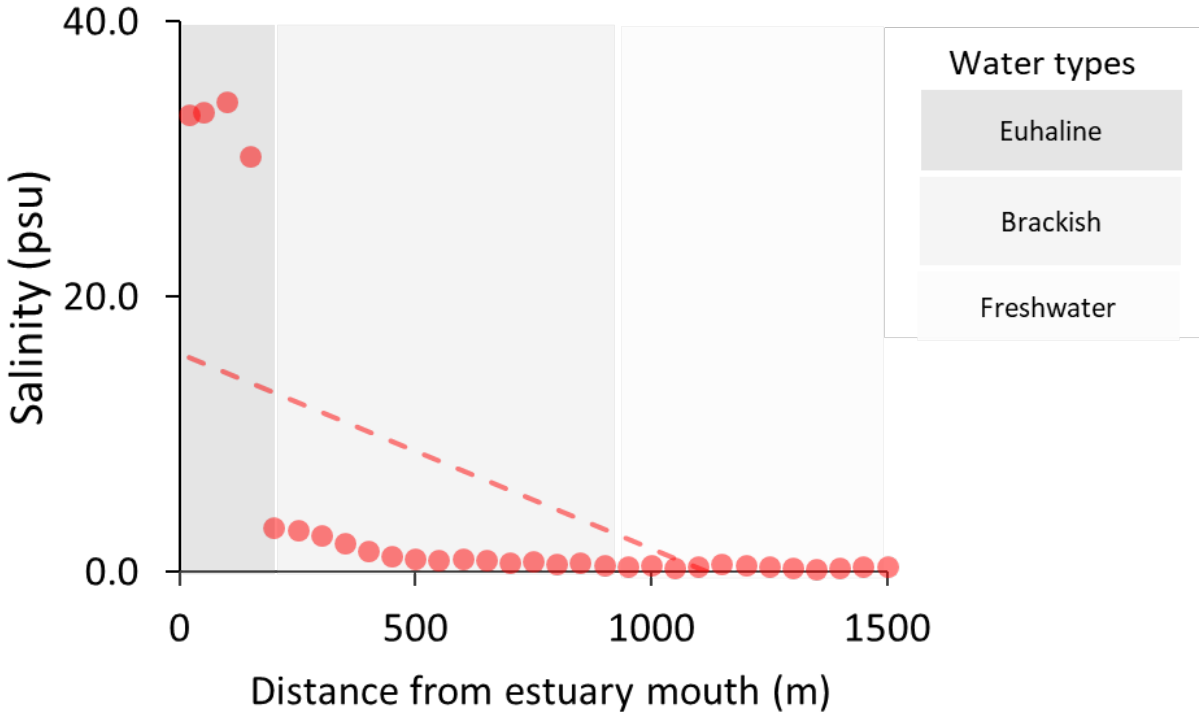

Figure 2. Salinity recorded along the Contaco Estuary. As expected, salinity values decrease significantly from the mouth to the head of the estuary ($r^2 = 0.382$, $P < 0.0001$). Three water types were identified in the Contaco Estuary based on salinity levels: euhaline (30–40 psu), brackish (0.5–29 psu), and fresh water (< 0.5 psu).

A total of 58,117 benthic foraminifera were identified, comprising 18,898 live individuals and 39,219 dead individuals. These individuals were distributed across 24 genera and 31 species, with eight agglutinated and 23 calcareous species identified (Table S1).

Species richness and diversity exhibited clear spatial and salinity-driven patterns along the Contaco Estuary. Richness declined progressively from the euhaline waters near the estuary mouth to the freshwater zones at its head, peaking at 24 species within the first 200 meters and decreasing to a minimum of two species between 1,250 and 1,550 meters (Figure 3a). Similarly, diversity, as measured by the Shannon-Wiener index, ranged from 1.8 to 0.6, with the highest values observed within the first 200 meters of the estuary. Beyond this range, diversity diminished alongside the decreasing salinity gradient, reaching its lowest levels in freshwater regions (Figure 3a).

Preprints.org (www.preprints.org) | NOT PEER-REVIEWED | Posted: 13 December 2024 doi:10.20944/preprints202412.1159.v1

Both richness and diversity were positively correlated with salinity, further underscoring the influence of the estuarine gradient on community structure. Richness displayed a strong positive correlation with salinity ($r^2 = 0.823$, $P < 0.0001$), while diversity followed a similar trend ($r^2 = 0.553$, $P < 0.0001$) (Figure 3b).

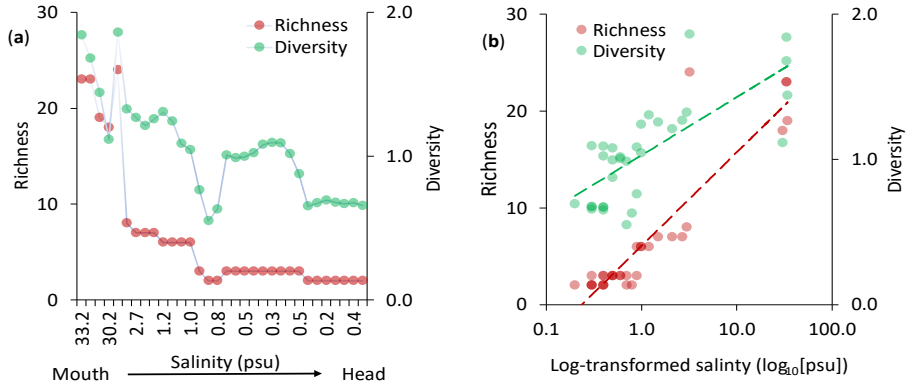

Figure 3. Species richness (number of species) and diversity (Shannon-Wiener diversity index) along the Contaco Estuary salinity gradient. (**a**) Species richness ranged from 24 to 2 species, while diversity ranged from 1.8 to 0.6. Both metrics showed a monotonic decrease from the estuary mouth to its head along with the observed salinity gradient. (**b**) Richness and diversity exhibited strong positive correlations with salinity: richness ($r^2 = 0.823$, $P < 0.0001$) and diversity ($r^2 = 0.553$, $P < 0.0001$). Panel (**a**) displays actual salinity values measured at ~50 m intervals along the estuary from mouth to head, while panel (**b**) illustrates the relationship between diversity metrics and log-transformed salinity values. These results highlight the influence of salinity on community composition and diversity patterns in the estuary.

3.2. Abundance Patterns

Total foraminiferal abundance in the Contaco Estuary exhibited a significant decrease from the mouth to the head of the estuary, following the observed salinity gradient (Figure 4a). Abundance fluctuated between a maximum of 1,578 individuals/10 cm³ at the estuary mouth, where salinity was highest (33.2 psu), and a minimum of 2 individuals/10 cm³ at the head of the estuary, where salinity dropped to 0.4–0.2 psu. This pattern reflects the dependence of foraminiferal taxa on salinity and their distinct tolerance ranges.

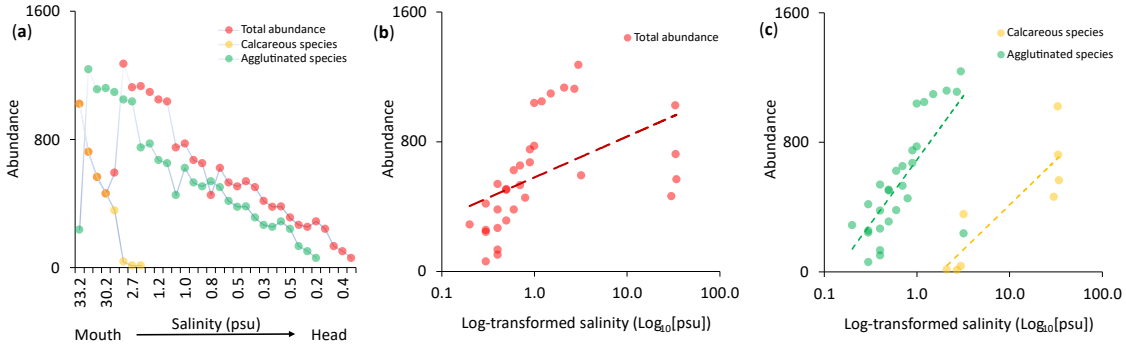

Figure 4. Spatial patterns and relationships between total, calcareous, and agglutinated foraminiferal abundance and salinity in the Contaco Estuary. (a) Total abundance, along with calcareous and agglutinated species, plotted against observed salinity (psu) measured from the estuary mouth to its head. The data reflect distinct tolerance levels, with calcareous species peaking in euhaline waters and agglutinated species in brackish waters. Notice the overlap between total abundance (red points) and calcareous species abundance (yellow points), resulting in orange points at the mouth of the estuary. (b) Relationship between total abundance and log-transformed salinity (log_{10}[psu]), showing a positive correlation ($r^2 = 0.239$, $P < 0.001$). (c) Abundance of calcareous and

 doi:10.20944/preprints202412.1159.v1

agglutinated species plotted against log-transformed salinity. Both groups show significant positive correlations with salinity: calcareous species (r^2 = 0.756, P < 0.0001) and agglutinated species (r^2 = 0.551, P < 0.0001).

Calcareous species reached their peak abundance (1,022 individuals/10 cm³) in euhaline waters near the estuary mouth, but their abundance declined sharply in brackish and freshwater zones, approaching near absence at salinities below 2 psu (Figure 4a). In contrast, agglutinated species showed a distinct pattern, peaking at 1,237 individuals/10 cm³ in brackish waters (2.7–1.0 psu) and gradually decreasing upstream to a minimum of 60 individuals/10 cm³ in freshwater zones (salinity < 0.5 psu) (Figure 4a). These contrasting patterns highlight the differential salinity tolerance of calcareous and agglutinated species.

When plotted against log-transformed salinity, total abundance exhibited a positive and significant correlation (r^2 = 0.647, P < 0.001; Figure 4b). Similarly, the abundance of calcareous and agglutinated species was strongly correlated with log-transformed salinity (r^2 = 0.934, P < 0.0001, and r^2 = 0.709, P < 0.0001, respectively; Figure 4c). The distribution of calcareous species was steeply associated with higher salinity values ($\log_{10}$[psu] > 1), reflecting their dependence on euhaline conditions, whereas agglutinated species were more evenly distributed across the salinity gradient, with a broader tolerance range.

Estuarine communities were dominated by four species, collectively accounting for 87% (n = 16,439 individuals) of the total abundance: *Ammonia* spp. (11%, 2,155 individuals), *Miliammina fusca* (42%, 7,941 individuals), *Trochamminita salsa* (29%, 5,391 individuals), and *Haplophragmoides wilberti* (5%, 952 individuals) (Figure 5a).

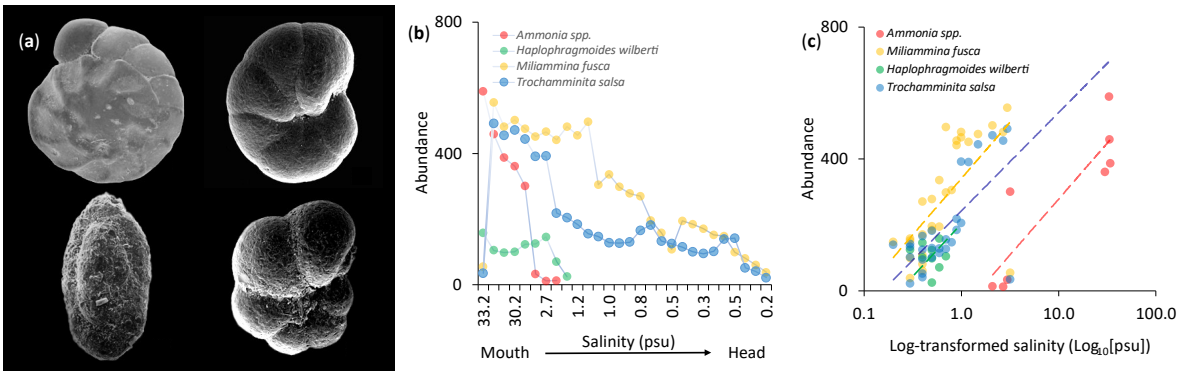

Figure 5. Relationships between the abundance of dominant foraminiferal species and salinity across the Contaco Estuary. (**a**) Scanning electron microscopy (SEM) images of the four dominant taxa, which account for 87% of the total abundance in the Contaco Estuary. Top row, from left to right: *Ammonia* spp. (calcareous) and *Haplophragmoides wilberti* (agglutinated). Bottom row, from left to right: *Miliammina fusca* (agglutinated) and *Trochamminita salsa* (agglutinated). (**b**) Longitudinal abundance patterns of the four dominant species along the observed salinity gradient, ranging from the estuary mouth (euhaline waters) to its head (freshwater). Each species shows a clear decrease in abundance upstream as salinity declines. Salinity values (psu) are plotted in their natural sequence, from highest to lowest, reflecting their actual longitudinal distribution along the estuarine gradient. The data highlight distinct salinity tolerance levels among taxa. (**c**) Abundance of the four dominant taxa as a function of log-transformed salinity ($\log_{10}$[psu]), with dashed lines representing regression fits for each taxon (*Ammonia* spp., r^2 = 0.779, P < 0.0001; *M. fusca*, r^2 = 0.439, P < 0.0001; *H. wilberti*, r^2 = 0.234, P < 0.0001; *T. salsa*, r^2 = 0.472, P < 0.0001).

The dominant foraminiferal taxa exhibited distinct abundance patterns along the salinity gradient of the estuary, reflecting their varying tolerances to salinity from the mouth to head of the estuary (Figure 5b). *Ammonia* spp. was the only calcareous taxon and showed a sharp decline in abundance towards the head, with its highest densities recorded near the estuary mouth in euhaline waters (33.2–30.2 psu) and becoming nearly absent beyond brackish zones. *M. fusca*, an agglutinated

 doi:10.20944/preprints202412.1159.v1

species, peaked in abundance in the brackish regions (around 2.7–1.2 psu) and demonstrated a gradual decline moving upstream. *T. salsa* maintained relatively consistent abundance levels in the brackish and freshwater sections of the estuary, showing a gradual decline towards the head. In contrast, *H. wilberti* exhibited moderate abundances in the brackish zone but persisted in lower salinity areas, including the freshwater region, indicating its greater tolerance to reduced salinity compared to the other taxa. Together, these patterns highlight a clear longitudinal distribution driven by salinity gradients and species-specific tolerances.

The abundance of the four dominant foraminiferal taxa demonstrated significant positive correlations with salinity (Figure 5c). *Ammonia* spp. exhibited the strongest correlation ($r^2 = 0.779$, $P < 0.0001$), with higher abundances observed at elevated salinity levels. Among the agglutinated species, *M. fusca showed* a moderate correlation with salinity ($r^2 = 0.439$, $P < 0.0001$), with abundances progressively increasing with salinity. *T. salsa* displayed a similar trend, with a slightly higher correlation ($r^2 = 0.472$, $P < 0.0001$). In contrast, *H. wilberti* showed the weakest correlation with salinity ($r^2 = 0.234$, $P < 0.0001$). These patterns highlight distinct ecological niches and tolerances among the taxa, with calcareous species thriving in higher salinity environments and agglutinated species demonstrating varying degrees of adaptability to lower salinity conditions.

3.3. Sampling Artifact Analysis

Rarefaction and extrapolation curves generated using iNEXT demonstrated that the sampling effort was effective in capturing the majority of species diversity across estuarine sites (Figures 6 and S1). The rarefaction curves indicated that species diversity reached clear asymptotes at most sites, reflecting comprehensive sampling coverage. While the extrapolation curves extended beyond observed values, the narrow confidence intervals for most sites underscored the robustness of the data and the reliability of species diversity estimates. These findings highlight the efficacy of the sampling strategy in accurately characterizing local species richness and community structure along the estuarine gradient, providing a solid foundation for subsequent analyses.

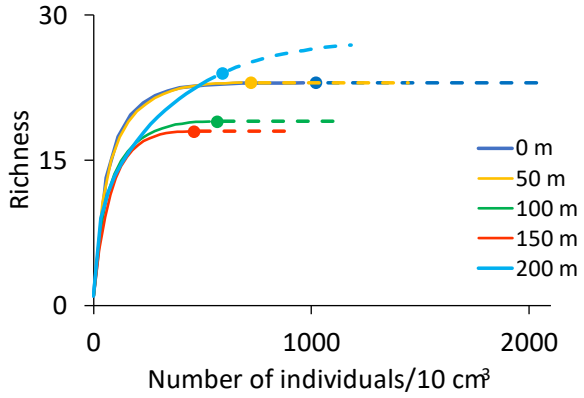

Figure 6. Rarefaction and extrapolation curves estimated using abundance data of foraminifera from the Contaco Estuary. To facilitate visualization, only the curves for the first five sampling sites (0, 50, 100, 150, and 200 m from the estuary mouth) are shown. Full rarefaction and extrapolation curves, including confidence intervals for all 32 sites, are available in the Figure S1. Solid lines represent rarefaction, while dashed lines indicate extrapolation. Circles along the curves denote the observed species richness based on the total number of individuals collected at each site. The x-axis reflects the number of individuals per 10 cm^3, and the y-axis indicates species richness. These results demonstrate effective sampling coverage, with most sites approaching an asymptote in species richness before extrapolation.

3.4. Rapoport's Rule and Mid-Domain Effect

A significant positive correlation between species range extent and range midpoint ($r^2 = 0.645$, $P < 0.0001$; Figure 7a) provided strong evidence for the presence of a longitudinal Rapoport's rule in the Contaco Estuary. This pattern suggests that foraminiferal species occurring further upstream

 doi:10.20944/preprints202412.1159.v1

exhibit broader distribution ranges than those at the estuary mouth, likely reflecting adaptations to greater environmental variability and stress near the estuarine head.

We did not found evidence supporting the occurrence of a mi-domain effect (MDE) in the Contaco Estuary. Observed species richness diverged significantly from the hump-shaped richness pattern predicted by the MDE null model (Figure 7b). Notably, only 34% of the observed richness values fell within the model's 95% confidence intervals, and the predicted peak in richness did not correspond to the empirical data. These findings suggest that factors other than geometric constraints, such as environmental gradients or ecological processes, are likely driving the observed patterns of species richness in the estuary.

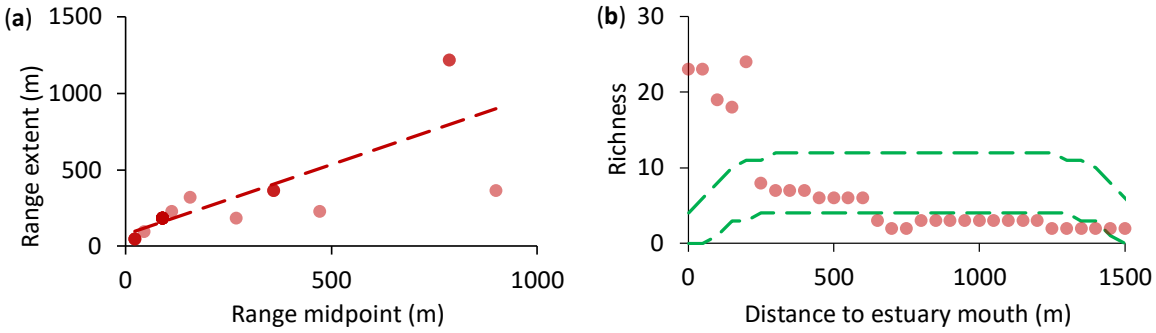

Figure 7. (**a**) Rapoport's rule: A significant positive relationship between range extent and range midpoint for the 31 species recorded ($r^2 = 0.645$, $P < 0.0001$) supports the existence of a longitudinal Rapoport's rule in the Contaco Estuary. The number of visible data points is smaller than the actual number due to overlapping values i.e., darker red points represent higher overlap density. (**b**) Mid-domain effect: Observed species richness (red circles) as a function of distance from the estuary mouth compared to the richness predicted by the upper and lower 95% confidence intervals of the mid-domain effect null model (green dashed lines). The empirical richness pattern diverged from the hump-shaped richness pattern predicted by the null model.

3.6. TA-Pattern vs. Source-Sink Dynamics

Beta diversity ($\beta_{SOR} = 0.921$) in the Contaco Estuary was primarily driven by turnover ($\beta_{SIM} = 0.743$), with nestedness ($\beta_{SNE} = 0.178$) contributing minimally (Figure 8a). These findings indicate that species replacement rather than species loss explains the longitudinal variation in foraminiferal communities. Hierarchical clustering (Figure 8b) and NMDS (Figure 8c) revealed only two main community groups rather than the three predicted by the TA-pattern (euhaline, brackish, and freshwater communities). ANOSIM results further confirmed the significance of the two identified clusters (global $R = 0.965$, $P < 0.0001$), but did not support the existence of three benthic foraminiferal communities. Species richness modeling highlighted a significant peak in observed richness at the estuary's mouth compared to null model expectations (Figure 8d). This peak likely represents a transitional zone where calcareous and agglutinated species co-occur. The narrow spatial extent of this potential ecotone may explain its undetectability through clustering and ordination analyses. Together, these results support the dominance of the TA-pattern but reveal deviations from its classical predictions due to the estuary's environmental constraints.

 doi:10.20944/preprints202412.1159.v1

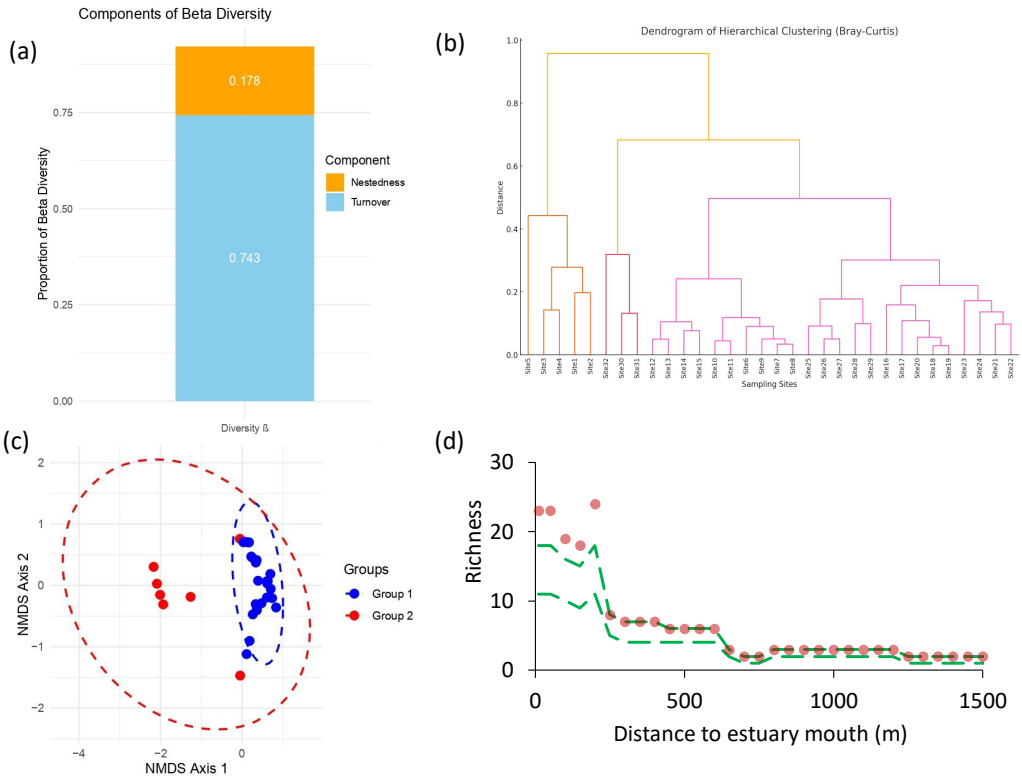

Figure 8. Summary of beta diversity components, clustering, NMDS, and species richness modeling results for benthic foraminiferal communities in the Contaco Estuary. (**a**) Beta diversity (β_{SOR} = 0.921) is primarily driven by turnover (β_{SIM} = 0.743) rather than nestedness (β_{SNE} = 0.178), indicating that species replacement dominates the spatial variation in community composition. (**b**) A Bray-Curtis clustering analysis identifies two distinct groups of sampling sites, aligning with the results of the NMDS. (**c**) Non-metric multidimensional scaling (NMDS) ordination confirms the presence of two discrete communities, as highlighted by 95% confidence ellipses. (**d**) Species richness modeling in PAST shows a peak of observed richness significantly higher than the null model prediction at the estuary's mouth. This peak likely represents a transitional zone where calcareous and agglutinated species co-occur, forming a central community predicted by the TA-pattern. However, the narrow spatial extent of this ecotone may render it undetectable in clustering and ordination analyses. Together, these findings suggest the presence of two main communities rather than the three predicted by the TA-pattern.

4. Discussion

The observed patterns in the Contaco Estuary offer valuable insights into the spatial distribution of protist diversity, particularly benthic foraminifera, along environmental gradients. Beyond the richness, diversity, and abundance trends discussed earlier, our findings also provide novel evidence supporting key biogeographical patterns, including the Rapoport's rule, and highlight the implications of null model analyses for understanding community assembly processes in estuarine systems.

4.1. Diversity and Richness Along the Estuarine Gradient

The species richness and diversity of benthic foraminifera in the Contaco Estuary were relatively low, a finding consistent with reports for macroorganisms and protists inhabiting estuarine systems worldwide. The observed richness values, ranging from 23 (near the estuary mouth) to 2 species (near its head), and diversity values, ranging from 1.8 to 0.6, align with previous studies in other southeastern Pacific estuaries [24,25,27] and elsewhere [3,4,19,20,22]. This reinforces the idea that the dynamic and stressful conditions in estuarine environments, such as fluctuating salinity, among others, act as strong environmental filters, limiting biodiversity [18,19,21].

 doi:10.20944/preprints202412.1159.v1

The monotonic decrease in richness and diversity from the euhaline waters at the estuary mouth to the freshwater head was strongly correlated with the salinity gradient. This trend corroborates the pivotal role of salinity in shaping estuarine biodiversity, as reported in studies of estuaries across different climatic and geographical contexts [17,23,27,34]. Similar patterns have been observed in other estuaries, where salinity gradients have been shown to drive longitudinal diversity patterns in macrofaunal and microbial communities [3,5,9,17,23,27,34].

4.2. Abundance and Salinity Tolerance

The total abundance of benthic foraminifera also decreased monotonically along the estuary, with a strong positive correlation with salinity. This pattern was evident across all dominant taxa, including *Ammonia* spp., *M. fusca*, *T. salsa*, and *H. wilberti*, which collectively represented 87% of the total abundance. *Ammonia* spp., a calcareous taxon, exhibited the highest abundance in the euhaline waters near the estuary mouth and declined significantly in brackish and freshwater environments. Conversely, the agglutinated taxa demonstrated broader salinity tolerances, with *M. fusca* and *T. salsa* dominating in brackish waters and persisting into the freshwater zones. This pattern of abundance, illustrating the transition from dominance by calcareous taxa to agglutinated taxa, is commonly observed in estuaries [17,18,23,24,27]. However, in our study site, the transition among calcareous and agglutinated communities appears more abrupt compared to the gradual shift typically reported in other estuarine systems. This discrepancy could be attributed to the Coastal Range, a prominent mountain range running parallel to the coastline, where numerous rivers originate. In the Los Lagos Region, this range reaches elevations of approximately 1,000 meters. The short distance between the Coastal Range and the sea results in steep gradients, causing rivers to flow rapidly as they discharge into the ocean. Combined with the region's high rainfall, this leads to a strong freshwater influence in the rivers, limiting marine intrusion into estuaries and preventing the formation of a well-defined transitional zone. [63].

The abundance patterns of the dominant taxa highlight distinct salinity tolerances and ecological niches. Calcareous taxa such as *Ammonia* spp. are highly dependent on calcium carbonate availability, limiting their distribution to high-salinity zones where carbonate saturation is sufficient for shell construction. In contrast, agglutinated taxa rely on sediment particles for shell construction and exhibit greater plasticity, enabling their persistence in low-salinity environments [9,10]. These findings align with global patterns reported in estuarine foraminiferal communities, where salinity tolerance determines species distribution and dominance [20,23,27,54].

4.3. Longitudinal Variation and Ecotonal Dynamics in Species Composition

Beta diversity in the Contaco Estuary was primarily driven by species turnover rather than nestedness, indicating that species replacement along the salinity gradient was more influential than species loss among sampling sites. This finding contradicts the predictions of source-sink dynamics, which typically emphasize nestedness as the dominant process shaping community composition [2,4,8,10]. Instead, the observed dominance of turnover supports the ecocline paradigm, which describes gradual changes in species composition along environmental gradients. Similar patterns of high turnover have been documented in other estuarine systems where salinity is a primary driver of biodiversity [20,23,27,54].

The salinity gradient and longitudinal variation in foraminiferal species composition observed in the Contaco Estuary align broadly with the TA-pattern. However, the TA-pattern predicts the formation of three discrete communities—marine, transitional, and freshwater—which were not distinctly observed. Instead, cluster, NMDS, and ANOSIM analyses supported the presence of two distinct communities: one associated with euhaline and brackish taxa and another dominated by brackish and freshwater taxa. This deviation from the TA-pattern likely stems from the estuary's steep salinity gradient and high freshwater input, which compress the brackish zone and limit the spatial extent of a well-defined transitional assemblage. Similar deviations have been reported in other small estuaries with steep environmental gradients [24,27].

 doi:10.20944/preprints202412.1159.v1

Null model analyses further revealed a peak in species richness near the euhaline-brackish transition zone, exceeding values predicted by chance. This localized increase in richness supports the presence of an ecotone where marine and brackish taxa co-occur. Ecotones often act as biodiversity hotspots due to overlapping species distributions from adjacent habitats [64]. However, the steep slope of the Contaco Estuary and the region's high precipitation likely compress the spatial extent of this ecotone, resulting in a transitional assemblage that is less detectable through community analysis methods.

The interplay between turnover and nestedness in shaping beta diversity highlights the coexistence of ecocline and ecotonal dynamics in the Contaco Estuary. While turnover predominates, the presence of nestedness—albeit to a lesser extent—suggests a complex assembly process influenced by both gradual environmental gradients and localized transitional zones. These findings emphasize the importance of scale-dependent approaches to understanding limnetic biodiversity and underscore the potential of aquatic environments as conservation priorities [65].

4.2. Rapoport's Rule and Mid-Domain Effect

This study provides the first evidence of the longitudinal Rapoport effect in estuarine protists, aligning with previous reports in terrestrial protists [11,35,37]. Specifically, the longitudinal range sizes of benthic foraminifera increased from the euhaline zone near the estuary mouth to the freshwater head. This pattern parallels findings in macroorganisms [2,5,66] and supports the hypothesis that species occupying environmentally suboptimal sites (e.g., freshwater zones for foraminifera) develop broader ecological tolerances and dispersal capacities. In this case, the greater salinity fluctuations and variability in the freshwater and brackish zones likely favored taxa with broader physiological tolerances, such as *H. wilberti* and *T. salsa*, which displayed larger longitudinal ranges compared to the calcareous *Ammonia* spp., confined to the euhaline zone.

The Rapoport's rule in protists extends a well-documented macroecological principle to microorganisms, emphasizing the shared influence of environmental variability on biodiversity across scales. This supports deterministic processes over stochasticity in shaping species distributions [3,6]. Such findings have implications for ecological modeling and biodiversity conservation, as they suggest that deterministic environmental gradients, like salinity, exert strong selective pressures on species' ranges.

Interestingly, the observed patterns deviate from the mid-domain effect (MDE), which predicts a hump-shaped richness distribution along gradients due to geometric constraints [6]. Instead, our results showed a monotonic decline in richness and diversity, with no peak at intermediate salinity levels. This finding underscores the limited role of stochastic geometric constraints (as predicted by the MDE) and the dominant influence of deterministic factors, such as salinity, in structuring benthic foraminiferal communities.

5. Conclusions

The findings of this study emphasize the importance of deterministic processes in structuring estuarine protist communities, while also revealing the nuanced interplay between ecocline and ecotonal dynamics. The first documentation of the Rapoport effect in estuarine protists highlights shared ecological principles governing the biogeography of macro- and microorganisms. These findings contribute to a growing body of evidence supporting the deterministic role of environmental gradients in shaping biodiversity, with implications for ecosystem monitoring, conservation, and management.

By bridging biogeographic theory and estuarine ecology, this study provides a robust framework for understanding and predicting biodiversity patterns in estuarine environments. The insights gained here extend beyond foraminifera, offering a valuable perspective for studying other microbial and macro-organism communities in similarly dynamic ecosystems.

Supplementary Materials: The following supporting information can be downloaded at: Preprints.org, Table S1: Distribution and abundance of benthic foraminiferal species along the longitudinal gradient of the Contaco

 doi:10.20944/preprints202412.1159.v1

Estuary; Figure S1: Rarefaction and extrapolation curves for benthic foraminiferal diversity across the 32 sampling sites in the Contaco Estuary, estimated using the package iNEXT.

Author Contributions: Author Conceptualization, L.D.F.; methodology, L.D.F.; formal analysis, L.D.F.; investigation, L.D.F. and M.M.; data curation, L.D.F. and M.M.; writing—original draft preparation, L.D.F. and M.M.; writing—review and editing, L.D.F. and M.M.; project administration, L.D.F.; funding acquisition, L.D.F. All authors have read and agreed to the published version of the manuscript.

Funding: This research was funded by ANID-FONDECYT Regular project number 1220605 granted to L.D. Fernández.

Institutional Review Board Statement: Not applicable.

Informed Consent Statement: Not applicable.

Data Availability Statement: All data collected during the course of this study are available within the manuscript or as supplementary material.

Acknowledgments: We thank Antonio Parra Gomez for generating the map used in Figure 1.

Conflicts of Interest: The authors declare no conflicts of interest.

References

1. Mittelbach, G.G.; Schemske, D.W.; Cornell, H.V.; et al. Evolution and the latitudinal diversity gradient: speciation, extinction and biogeography. *Ecol. Lett.* **2007**, *10*, 315–331. https://doi.org/10.1111/j.1461-0248.2007.01020.x.
2. Hernández, C.E.; Moreno, R.A.; Rozbaczylo, N. Biogeographical patterns and Rapoport's rule in southeastern Pacific benthic polychaetes of the Chilean coast. *Ecography* **2005**, *28*, 363–373.
3. Dunn, R.R.; Colwell, R.K.; Nilsson, C. The river domain: why are there more species halfway up the river? *Ecography* **2006**, *29*, 251–259.
4. Moreno, R.A.; Rivadeneira, M.M.; Hernández, C.E.; Sampértegui, S.; Rozbaczylo, N. Do Rapoport's rule, the mid-domain effect or the source-sink hypotheses predict bathymetric patterns of polychaete richness on the Pacific coast of South America? *Glob. Ecol. Biogeogr.* **2008**, *17*, 415–423.
5. Beketov, M.A. The Rapoport effect is detected in a river system and is based on nested organization. *Glob. Ecol. Biogeogr.* **2009**, *18*, 498–506.
6. McCain, C.M. Global analysis of bird elevational diversity. *Glob. Ecol. Biogeogr.* **2009**, *18*, 346–360. https://doi.org/10.1111/j.1466-8238.2008.00443.x.
7. Wiens, J.J.; Ackerly, D.D.; Allen, A.P.; Anacker, B.L., Buckley, L.B.; Cornell, H.V.; Damschen, E.I.; Jonathan Davies, T.; Grytnes, J.A.; Harrison, S.P.; Hawkins, B.A.; Holt, R.D.; McCain, C.M.; Stephens, P.R. Niche conservatism as an emerging principle in ecology and conservation biology. *Ecol. Lett.* **2010**, *13*, 1310–1324. https://doi.org/10.1111/j.1461-0248.2010.01515.x.
8. Almeida-Neto, M.; Ulrich, W. A straightforward computational approach for quantifying nestedness using abundance data. *Environ. Modell. Softw.* **2011**, *26*, 173–178.
9. El Yaagoubi, S.; Edegbene, A.O.; El Haissoufi, M.; Harrak, R.; El Alami, M. Odonata, Coleoptera, and Heteroptera (OCH) Trait-Based Biomonitoring of Rivers within the Northwestern Rif of Morocco: Exploring the Responses of Traits to Prevailing Environmental Gradients. *Ecologies* **2024**, *5*, 132–154. https://doi.org/10.3390/ecologies5010009.
10. Fernández, L.D. Source–sink dynamics shapes the spatial distribution of soil protists in an arid shrubland of northern Chile. *J. Arid Environ.* **2015**, *113*, 121–125. https://doi.org/10.1016/j.jaridenv.2014.10.007.
11. Fernández, L.D.; Fournier, B.; Rivera, R.; et al. Water–energy balance, past ecological perturbations and evolutionary constraints shape the latitudinal diversity gradient of soil testate amoebae in south-western South America. *Glob. Ecol. Biogeogr.* **2016**, *25*, 1216–1227. https://doi.org/10.1111/geb.12478.
12. Schiaffino, M.R.; Lara, E.; Fernández, L.D.; et al. Microbial Eukaryote Communities Exhibit Robust Biogeographical Patterns along a Gradient of Patagonian and Antarctic Lakes. *Environ. Microbiol.* **2016**, *18*(12), 5249–5264. https://doi.org/10.1111/1462-2920.13565.
13. Fernández, L.D.; Hernández, C.E.; Schiaffino, M.R.; Izaguirre, I.; Lara, E. Geographical Distance and Local Environmental Conditions Drive the Genetic Population Structure of a Freshwater Microalga (Bathycoccaceae; Chlorophyta) in Patagonian Lakes. *FEMS Microbiol. Ecol.* **2017**, https://doi.org/10.1093/femsec/fix125.
14. Geisen, S.; Mitchell, E.A.D.; Wilkinson, D.M.; et al. Soil protistology rebooted: 30 fundamental questions to start with. *Soil Biol. Biochem.* **2017**, *111*, 94–103. https://doi.org/10.1016/j.soilbio.2017.04.001.
15. Singer, D.; Mitchell, E.A.D.; Payne, R.J.; et al. Dispersal limitations and historical factors determine the biogeography of specialized terrestrial protists. *Mol. Ecol.* **2019**, *0*, https://doi.org/10.1111/mec.15117.

16. Adl, S.M.; Simpson, A.G.B.; Lane, C.E.; et al. The Revised Classification of Eukaryotes. *J. Eukaryot. Microbiol.* **2012**, *59*, 429–493. https://doi.org/10.1111/j.1550-7408.2012.00644.x.
17. Boltovskoy, E.; Lena, H. Foraminíferos del Río de la Plata. *Serv. Hidrogr. Naval.* **1974**, *661*, 3–22.
18. Scott, D.B.; Medioli, F.S. Quantitative studies of marsh foraminiferal distributions in Nova Scotia: Implications for sea level studies. *J. Foraminiferal Res.* **1980**, *17*, 58.
19. Boltovskoy, E.; Giussani, G.; Watanabe, S.; Wright, R. Atlas of benthic shelf foraminifera of the southwest Atlantic. *Junk by Publications: London, UK,* **1980**.
20. Hayward, B.W.; Grenfell, H.R.; Reid, C.M.; Hayward, K.A. Recent New Zealand shallow-water benthic foraminifera: taxonomy, ecologic distribution, biogeography, and use in paleoenvironmental assessment. *Institute of Geological and Nuclear Sciences Monograph 21: Lower Hutt, New Zealand,* **1999**.
21. Scott, D.B.; Medioli, F.S.; Schafer, C.T. Monitoring in Coastal Environments Using Foraminifera and Thecamoebian Indicators. *Cambridge University Press: Cambridge, UK,* **2001**.
22. Murray, J.W. Ecology and applications of benthic foraminifera. *Cambridge University Press: Cambridge, UK,* **2006**.
23. Wang, P. Distribution of foraminifera in estuarine deposits: a comparison between Asia, Europe, and Australia. In *Centenary of Japanese Micropaleontology*; Ishizaki, K., Saito, T., Eds.; *Terra Scientific Publishing Company: Tokyo, Japan,* **1992**; pp. 71–83.
24. Zapata, J.; Álvarez, P.; Cea, C. Tecamebas del Río Contaco (40°33′12″ S; 73°43′00″ W), Osorno, Chile. *Bol. Soc. Biol. Concepción* **2002**, *73*, 17–35.
25. Fernández, L. Foraminíferos (Protozoa: Foraminiferida) del estuario del río Contaco (40°33′S; 73°43′O), Chile. *Bol. Biodivers. Chile* **2010**, *4*, 18–62.
26. Fernández, L.; Zapata, J. Registro tafonómico de *Ammonia beccarii* (Linné, 1758) (Protozoa: Foraminiferida) en la ensenada Quillaipe (41° 32′ S; 72° 44′ O), Chile. *Lat. Am. J. Aquat. Res.* **2010**, *38*, 286–291.
27. Fernández, L.; Zapata, J. Distribution of benthic foraminifera (Protozoa: Foraminifera) in the Quillaipe Cove (41°32′ S; 72°44′ W), Chile: Implications for sea level studies. Rev. Chil. Hist. Nat. **2010**, 83, 567–583. https://doi.org/10.4067/S0716-078X2010000400010.
28. Stevens, G.C. The latitudinal gradient in geographical range: How so many species coexist in the tropics. Am. Nat. **1989**, 133, 240–256.
29. Stevens, G.C. Extending Rapoport's rule to Pacific marine fishes. J. Biogeogr. **1996**, 23, 149–154.
30. Pulliam, H.R. Sources, sinks, and population regulation. Am. Nat. **1988**, 132, 652–661.
31. Almeida-Neto, M.; Guimarães, P.; Guimarães, P.R. Jr.; Loyola, R.D.; Ulrich, W. A consistent metric for nestedness analysis in ecological systems: Reconciling concept and measurement. Oikos **2008**, 117, 1227–1239.
32. Colwell, R.K.; Lees, D.C. The mid-domain effect: Geometric constraints on the geography of species richness. Trends Ecol. Evol. **2000**, 15, 70–76. https://doi.org/10.1016/S0169-5347(99)01767-X.}
33. Xu, M.; Du, R.; Li, X.; et al. The mid-domain effect of mountainous plants is determined by community life form and family flora on the Loess Plateau of China. Sci. Rep. **2021**, 11, 10974. https://doi.org/10.1038/s41598-021-90561-4.
34. Hewson, I.; Fuhrman, J.A. Richness and diversity of bacterioplankton species along an estuarine gradient in Moreton Bay, Australia. Appl. Environ. Microbiol. **2004**, 70, 3425–3433.
35. Fernández, L.D.; Seppey, C.V.W.; Singer, D.; Fournier, B.; Tatti, D.; Mitchell, E.A.D.; Lara, E. Niche conservatism drives the elevational diversity gradient in major groups of free-living soil unicellular eukaryotes. Microb. Ecol. **2022**, 83, 459–469. https://doi.org/10.1007/s00248-021-01771-2.
36. Fernández, L.D.; Lara, E.; Mitchell, E.A.D. Checklist, diversity and distribution of testate amoebae in Chile. Eur. J. Protistol. **2015**, 51, 409–424. https://doi.org/10.1016/j.ejop.2015.07.001.
37. Campello-Nunes, P.H.; Woelfl, S.; da Silva-Neto, I.D.; da S. Paiva, T.; Fernández, L.D. Checklist, diversity and biogeography of ciliates (Ciliophora) from Chile. Eur. J. Protistol. **2022**, 84, 125892. https://doi.org/10.1016/j.ejop.2022.125892.
38. Zapata, J.; Zapata, C.; Gutiérrez, A. Foraminíferos bentónicos recientes del sur de Chile. Gayana Zool. **1995**, 59, 25–40.
39. Zapata, J.; Moyano, H. Distribution of benthic foraminifera collected by the Akebono Maru "72" in southern Chile. Gayana Zool. **1996**, 60, 89–98.
40. Zapata, J.; Moyano, H. Foraminíferos bentónicos recientes de Chile Austral. Bol. Soc. Biol. Concepción **1997**, 68, 27–37.
41. Zapata, J. Foraminíferos bentónicos recientes de bahía Cumberland (33°41′S; 78°50′W), Archipiélago de Juan Fernández, Chile: Aspectos zoogeográficos. Bol. Soc. Biol. Concepción **1999**, 70, 21–35.
42. Marchant, M.; Hebbeln, D.; Wefer, G. High-resolution planktic foraminiferal record of the last 13,300 years from the upwelling area off Chile. Mar. Geol. **1999**, 161, 115–128. https://doi.org/10.1016/S0025-3227(99)00041-9.

43. Hromić, T. Distribución latitudinal de foraminíferos bentónicos (Protozoa: Foraminiferida) a nivel de subórdenes y familias, en canales y fiordos patagónicos chilenos. Invest. Mar. **2006**, 34, 71–81. http://dx.doi.org/10.4067/S0717-71782006000100006.
44. Hromić, T.; Ishman, S.; Silva, N. Hromić, T.; Ishman, S.; Silva, N. Benthic foraminiferal distributions in Chilean fjords: 47°S to 54°S. Mar. Micropaleontol. **2006**, 59, 115–134. https://doi.org/10.1016/j.marmicro.2006.02.001.
45. Marchant, M.; Hebbeln, D.; Giglio, S.; Coloma, C.; González, H.E. Seasonal and interannual variability in the flux of planktic foraminifera in the Humboldt Current System off central Chile (30°S). Deep-Sea Res. **2004**, 51, 2441–2455. https://doi.org/10.1016/j.dsr2.2004.08.013.
46. Hromić, T.; Montiel, A. Foraminíferos bentónicos de Seno Gallegos y Bahía Brookes (54.5°S - 69.5°S), Chile: Patrones de distribución y diversidad. An. Inst. Patagon. **2011**, 39, 33–46. http://dx.doi.org/10.4067/S0718-686X2011000200003.
47. Tavera Martínez, L.; Marchant, M.; Muñoz, P.; Abdala Díaz, R.T. Spatial and vertical benthic foraminifera diversity in the oxygen minimum zone of Mejillones Bay, northern Chile. Front. Mar. Sci. **2022**, 9, 821564. https://doi.org/10.3389/fmars.2022.821564
48. Tavera, L.; Fernández, L.; Marchant, M.; Hromic, T. The biogeography of benthic foraminifera is driven by ecological and historical processes in the Humboldt Current System-Southeastern Pacific. SSRN Preprint. https://doi.org/10.2139/ssrn.4992087.
49. Páez, M.; Zúñiga, O.; Valdés, J.; Ortlieb, L. Foraminíferos bentónicos recientes en sedimentos micróxicos de la bahía Mejillones del Sur (23º S), Chile. Rev. Biol. Mar. Oceanogr. **2001**, 36, 129–139. https://doi.org/10.4067/S0718-19572001000200002.
50. Schafer, C.T.; Scott, G.V.; Pocklington, D.B.; Cole, P.; Honig, C. Survey of living foraminifera and polychaete populations at some Canadian aquaculture sites: Potential for impact mapping and monitoring. J. Foraminiferal Res. **1995**, 25, 236–259.
51. Scott, D.B.; Medioli, F.S. Living vs. total foraminiferal populations: Their relative usefulness in paleoecology. J. Paleontol. **1980**, 4, 814–831.
52. Horton, B.P.; Edwards, R.J. Quantifying Holocene sea-level change using intertidal foraminifera: Lessons from the British Isles. J. Foraminiferal Res. **2006**, 40, 1–97.
53. Hammer, Ø.; Harper, D.; Ryan, P. PAST: Paleontological statistics software for education and data analysis. Paleontol. Electron. **2001**, 4, 1–9.
54. Boltovskoy, E. Distribution of recent foraminifera in the South America region. In Foraminifera; Hedley, R.H., Adams, C.G., Eds.; Academic Press: London, UK, **1976**; pp. 273–236.
55. Gotelli, N.; Entsminger, G. EcoSim: Null models software for ecology, version 7.72; Acquired Intelligence Incorporated and Kesey-Bear: Jericho, VT, USA, 2009.
56. Chao, A.; Gotelli, N.J.; Hsieh, T.C.; Sander, E.L.; Ma, K.H.; Colwell, R.K.; Ellison, A.M. Rarefaction and extrapolation with Hill numbers: A framework for sampling and estimation in species diversity studies. Ecol. Monogr. 2014, 84, 45–67.
57. Rohde, K.; Heap, M.; Heap, D. Rapoport's rule does not apply to marine teleosts and cannot explain latitudinal gradients in species richness. Am. Nat. **1993**, 142, 1–16.
58. McCain, C.M. The mid-domain effect applied to elevational gradients: Species richness of small mammals in Costa Rica. J. Biogeogr. **2004**, 31, 19–31.
59. Baselga, A.; Orme, C.D.L. betapart: An R package for the study of beta diversity. Methods Ecol. Evol. **2012**, 3, 808–812. https://doi.org/10.1111/j.2041-210X.2012.00224.x.
60. R Core Team. R: A language and environment for statistical computing; R Foundation for Statistical Computing: Vienna, Austria, 2023. Available online: https://www.R-project.org/.
61. Oksanen, J.; Blanchet, F.G.; Kindt, R.; Legendre, P.; Minchin, P.R.; O'Hara, R.B.; Simpson, G.L.; Solymos, P.; Stevens, M.H.H.; Wagner, H. Vegan: Community ecology package. R Package Version 2.2-0. 2014. Available online: http://CRAN.R-project.org/package=vegan.
62. Wickham, H. ggplot2: Elegant Graphics for Data Analysis; Springer-Verlag: New York, NY, USA, 2016. ISBN 978-3-319-24277-4. Available online: https://ggplot2.tidyverse.org.
63. Habit, E.; Belk, M.; Victoriano, P.; Jaque, E. Spatio-temporal distribution patterns and conservation of fish assemblages in a Chilean coastal river. Biodivers. Conserv. **2007**, 16, 3179–3191. https://doi.org/10.1007/s10531-007-9173-9.
64. Attrill, M.J.; Rundle, S.D. Ecotone or ecocline: Ecological boundaries in estuaries. Estuar. Coast. Shelf Sci. **2002**, 55, 929–936.
65. Lu, L.; Zhao, D.; Li, Z.; Fernández, L.D. Editorial: Microbial Diversity and Ecosystem Functioning in Fragmented Rivers Worldwide. Front. Microbiol. **2023**, 14. https://doi.org/10.3389/fmicb.2023.1253190.
66. Parra-Gómez, A.; Fernández, L.D. Filling gaps in the diversity and biogeography of Chilean millipedes (Myriapoda: Diplopoda). Arthropod Syst. Phylogeny **2022**, 80, 561–573. https://doi.org/10.3897/asp.80.e86810.

 doi:10.20944/preprints202412.1159.v1